Lithofacies Types and Reservoir Characteristics of Mountain Shale in Wufeng Formation-Member 1 of Longmaxi Formation in the Complex Structural Area of Northern Yunnan−Guizhou

Bingqiang Chai,* Feng Zhao, Yubing Ji, Lei Chen, and Qingsong Cheng

Cite This: *ACS Omega* 2023, 8, 2085−2097

Read Online

ACCESS | 📊 Metrics & More | 📖 Article Recommendations

ABSTRACT: The mountain shale in Wufeng Formation-Member 1 of Longmaxi Formation in the complex structural area of northern Yunnan−Guizhou has great potential for exploration and development. In order to clarify the differences of reservoir quality and the longitudinal distribution law of different lithofacies, the lithofacies in Wufeng Formation-Member 1 of Longmaxi Formation was divided combined with core, logging, and analytical test data. Based on the data of total organic carbon, laminate structure, reservoir porosity types and physical properties, and gas content, the reservoir characteristics and advantageous lithofacies shale reservoir distribution were determined. The results show that the mountain shale lithofacies in the study area are divided into 7 major types and 20 subtypes. The high-carbon siliceous shale has the highest degree of organic pore development, specific surface area (average 28.55 cm^2/g), and pore volume (average 0.0397 cm^3/g). Two types of advantageous lithofacies shale reservoir in the study area were identified. The high-carbon siliceous shale reservoir could be considered as an excellent shale reservoir for shale gas and is mainly concentrated in the first section. It is mainly developed in layer-1 and the bottom of layer-2 of the Longmaxi Formation, providing favorable source-reservoir conditions for shale gas enrichment. The medium-carbon siliceous shale, medium-carbon clay siliceous shale, and medium-carbon calcareous siliceous shale, developed in the top of layer-2 and the bottom of layer-3 of the Longmaxi Formation, are assumed to be moderately promising for shale gas. Therefore, the research results deepen the understanding of the longitudinal distribution of the dominant shale reservoirs in the study area and are of great significance in promoting strategic transfer of the main shale gas exploration system in the south from the Sichuan basin to the outer basin.
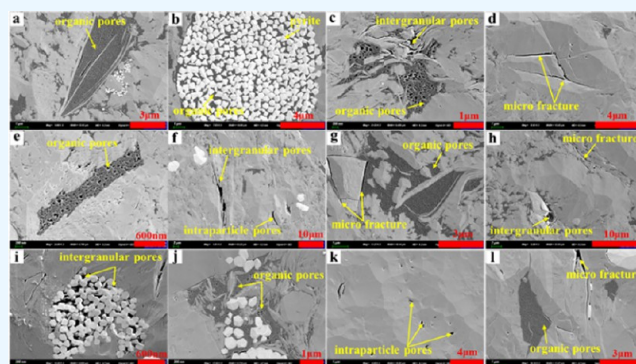
1. INTRODUCTION

Shale refers to fine-grained sedimentary rocks with particle size smaller than 63 μm and more than 50% mud (i.e., silt and clay) content, including mudstone, shale (narrow sense), claystone, siltstone, marl, calcareous layer, and many other rocks deposited in low-energy environments.[1] As the main venue for exploration and development of marine shale gas in China, the Sichuan basin and surrounding areas have established shale gas production bases such as Fuling, Changning, Weiyuan, and Zhaotong. The mountain shale in Wufeng Formation−Longmaxi Formation in the complex structural area of northern Yunnan and Guizhou at depths less than 3500 m is a key target for exploration and development.[2,3] Mountain shale refers to shale in tectonically active areas, controlled by small formations within shale formations, which is significantly different from conventional shale in terms of exploration and development.[4] The mountain shale is frequently hilly in surface topography as well as complex subsurface formations, with strong late tectonic effects and complex and diverse tectonic patterns, especially when the intra-

formational formations are inconsistent with regional tectonics.[5] The intraplate deformation caused by the superimposition of multiple mountain movements has characterized the area as "strongly tectonically altered, large petrographic changes, over-mature evolution, and high complex ground stress", which poses great difficulties and challenges for the exploration and development of shale gas in mountainous areas.[6] The mountain shale in the complex structure area in northern Yunnan−Guizhou differs significantly from the organic-rich shale in Wufeng Formation−Longmaxi Formation in the Sichuan Basin in terms of reservoir size, lithological characteristics, and gas-bearing properties.[7] Identifying the characteristics of the shale
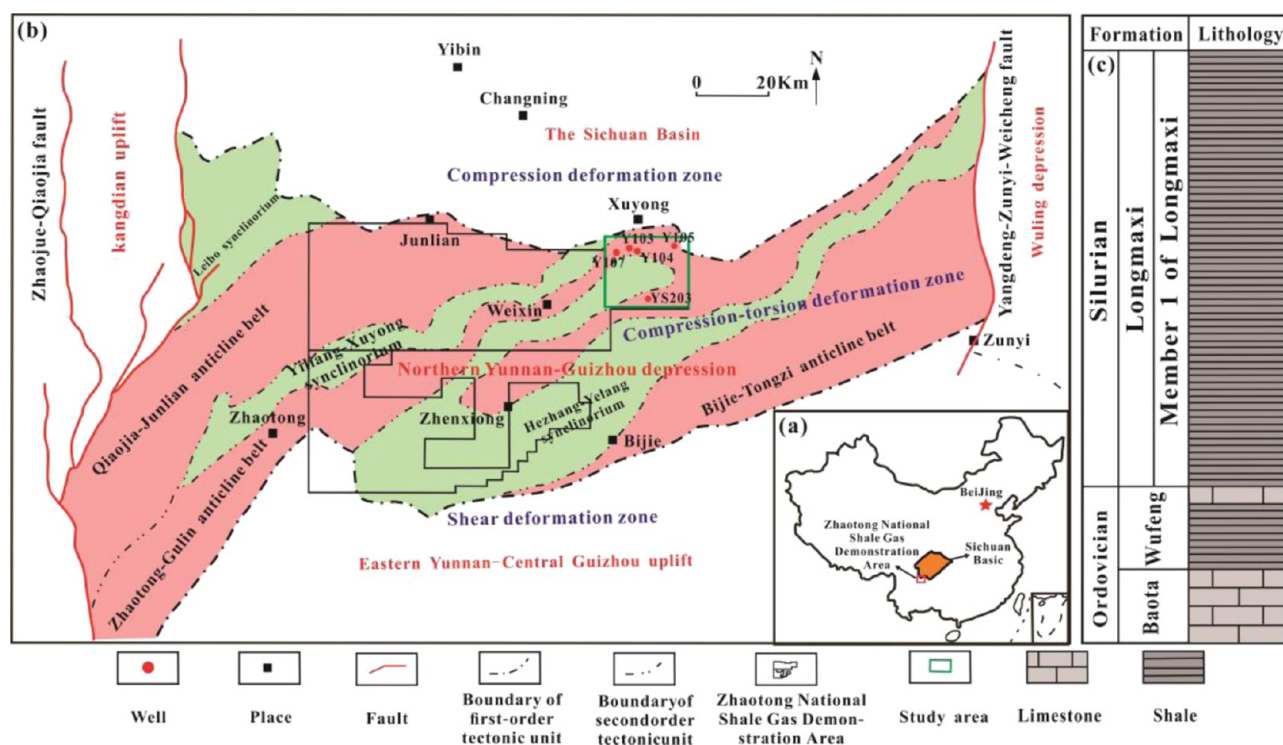
Figure 1. Location, tectonic setting, and stratigraphy of the study area. (a) Location of the Sichuan Basin and the study area. Reprinted (adapted or reprinted in part) with permission from Chen et al.[26] (b) tectonic setting and well location information of the study area. Reprinted (adapted or reprinted in part) with permission from Liang et al.[4] and (c) stratigraphic delight of the study area.

lithofacies and reservoirs in the study area is of great significance to deepen the geological understanding of shale gas enrichment and reservoir formation.

Lithofacies is the summation of rock types, lithology combination, and sedimentary structural characteristics formed in a specific sedimentary environment, which determines the distribution of shale sweet spots and controls the hydrocarbon generation capacity and reservoir performance of shale.[8,9] Lithofacies have evolved as a technical tool combining mineralogy, geochemistry, and geophysics to identify shale characteristics.[2,10] Extensive heterogeneity is observed in shale characteristics such as mineralogical composition, sedimentary architecture, and pore structure among the different petrographic shales. The scheme of lithofacies division, the selection of characteristic parameters of lithofacies division, and the classification threshold have always been the key contents discussed and studied by experts and scholars.[11] An excessively detailed lithofacies division scheme will not only lead to excessive non-homogeneity in the longitudinal direction and poor continuity in the lateral direction of the shale but will also make the variation pattern of reservoir parameters such as pore structure incompatible with the lithofacies type and unsuitable for practical production.[12] The reservoir parameters of different lithofacies shale are different. By systematically analyzing the characteristics of reservoir space and gas content of different shale lithofacies, it can provide reference for accurate identification of shale sweet spots.[13] However, there are still some shortcomings in the study of lithofacies division and reservoir characteristics. For example, when the lithofacies is divided based on mineral composition, the mixed lithofacies is not further finely divided, resulting in the poor characterization of the differences in reservoir parameters of each lithofacies. At present, there are mainly two lithofacies division schemes for

marine shales. One is based on the three-end-member method (using mineral components),[14] which fails to take total organic carbon (TOC) into account and cannot fully characterize the shale reservoir. The other is to classify the lithofacies type based on the difference in mineral composition and TOC,[15] although the values of the TOC division critical points in this scheme are not the same. It should be noted that the marine shale lithologies are finely classified mainly in the southern and eastern Sichuan Basin. There are few studies related to mountain shale in the complex structural area of northern Yunnan−Guizhou, with only Chen[16] identifying six lithofacies types in the lower part of the Wufeng Formation−Longmaxi Formation in northern Yunnan−Guizhou on the basis of the mineral three-end-member method. Li[17] combined shale TOC and mineral components to classify the shales in the Wufeng Formation−Longmaxi Formation of northern Yunnan−Guizhou into nine lithofacies types, and two limitations in his study are as follows: (1) it merely uses 2% as the TOC classification threshold to classify shales into carbon-rich and carbon-poor shales, without further refinement; and (2) it simply focuses on 35 shale samples collected from five wells, a limited number of samples, and it is questionable whether his research results are representative.

The Taiyang shale gas field in the complex structural area of north Yunnan−Guizhou has obtained proven shale gas reserves of 2576.35×10^8 m^3 until 2021.[18] To further foster the exploration and development of mountain shale gas in the study area, a more detailed study of the shale lithofacies using new well data is essential. In this article, with the combination of the three-end-member method (using mineral components) and TOC, lithofacies types of mountain shale in Wufeng Formation-Member 1 of Longmaxi Formation in the complex structural area of northern Yunnan−Guizhou were identified. A comprehensive analysis of the reservoir development character-

istics in the major lithofacies by integrating the laminate structure, reservoir space and physical properties, and gas-bearing properties was carried out. Three key parameters, namely TOC content, siliceous mineral content, and clay mineral content, were selected to establish the classification criteria for the dominant lithologies and the favorable shale lithofacies were identified for exploration and development. The research results will be a reference for the exploration and development of shale gas in the complex structural areas of north Yunnan−Guizhou and promote the strategic transfer of the main shale gas exploration system in the south from within the Sichuan Basin to outside the basin.

2. GEOLOGICAL SETTING

The main body of the study area is located in the Taiyang anticline tectonic area in the northeast of Zhaotong demonstration area, which is located in the transition part between Zhaotong−Guilin anticline belt and Hengzhang-Yelang synclinorium in northern Yunnan−Guizhou depression (Figure 1a,b).[19] The Taiyang anticline is characterized by east−west distribution, high in the south and low in the north, and steep in the north and gentle in the south. Affected by the activity of NW and NE trending compressive strike-slip faults, the attitude of the nearly EW-trending strata in the Taiyang anticline changes gently, the faults at the top of the anticline are relatively undeveloped, and the anticline structure is relatively simple. The footwall of the faults in the south and north wings develops nearly EW trending trough belts, which are complicated by faults.[20] During the Ordovician period, the tectonic-depositional environment in the study area was relatively stable, and as sea level continued to rise, the Yangzi plate formed extensive shallow marine terraces, depositing limestones of the Baota Formation and black shales of the Wufeng Formation (Figure 1c). In the Early Silurian period, extensive sea erosion occurred resulting from the end of the Gondwana continental ice age, and a suite of black shales was deposited in the Longmaxi Formation at the bottom of the Silurian. The main body of the Wufeng−Longmaxi Formation is a black shale formed in the northern foreland basin belt, controlled and occluded by the Garridon orogenic belt in South China, which belongs to the anoxic depositional environment of the stagnant basin, with a thickness mostly distributed in the range of 200−350 m.[21] The main lithofacies of the Longmaxi Formation is the black shales. Based on the sedimentary cyclonic characteristics, the Longmaxi Formation can be divided into Member 1 and Member 2. Member 2 of Longmaxi Formation mainly develops gray shales with slightly higher organic matter content, less penstones, and small individuals at the bottom. Member 1 of Longmaxi Formation is subdivided into Long 1 submember-1 and Long 1 submember-2. Long 1 submember-1 is dominated by deep-water shelf phase deposits, developing black siliceous shales and carbonaceous shales, with common pyrite nodules and penstones. These transition to semi-deep water shelf phase deposits upward to the Long 1 submember-2, over 100 m thick, with gray and black shale dominating the lithology.[22−25]

3. SAMPLES AND METHODS

3.1. Samples. The samples used in this study are all from five drilled wells (Y103, Y105, Y104, Y107, and YS203) in the complex structural area of northern Yunnan−Guizhou (Figure 1a), with a total of 155 mountain shale samples, belonging to the Wufeng Formation-Member 1 of Longmaxi Formation. Experi-

ments (TOC, X-ray diffraction (XRD), and N_2 gas adsorption analysis) were carried out in the State Key Laboratory of Oil and Gas Reservoir Geology and Exploitation, Southwest Petroleum University. FE-SEM experiment was completed by the experimental center of School of Geoscience and Technology, Southwest Petroleum University. Shale gas content test was conducted by Langfang Branch of Exploration and Development Research Institute of China National Petroleum Corporation, Unconventional oil and gas experimental center.

3.2. Experimental Methods. *3.2.1. XRD and TOC.* According to the Chinese national standard (SY/5163-2018) and using an X'Pert PRO X-ray diffractometer, XRD was performed. Before the experiment, shale samples were milled to 200 mesh. The experiment was carried out under the conditions of 35 kV tube voltage, 30 mA tube current, scanning range $2\theta = 5−90°$, and a scanning speed of $10°/min$.

The TOC experiment was conducted using a multi N/C 3100 type tester according to the Chinese industry standard (GB/T 19145-2003). Before the experiment, the samples were introduced into a persulfate reactor and a phosphoric acid reactor to decompose organic compounds and inorganic carbonate into CO_2, which was blown out by high-purity nitrogen and dehumidified by a drying tube before entering a non-dispersive infrared detector. Based on the ratio of carbon content between CO_2 and TOC, total carbon (TC) and inorganic carbon (IC) were measured. The difference between TC and IC is the TOC.

3.2.2. N₂ Gas Adsorption Analysis. The low-pressure N_2 gas adsorption experiment was conducted in accordance with the Chinese national standard (GB/T 5751-2009), and the Nova 2000e automatic N_2 adsorption instrument (Quantachrome Company, Boynton Beach, FL) was used. The samples were prepared into particles of about 3 mm and then dried at 110 °C for 24 h for degassing. After naturally cooling down, N_2 gas was used as an adsorption gas to obtain the adsorption and desorption isotherm. The Brunauer−Emmett−Teller (BET) model was used to calculate the specific surface area, and the Barret−Joyner−Halenda (BJH) model was applied to calculate the pore volume and pore size distribution based on N_2 adsorption data, which could effectively characterize the pore distribution characteristics of mesopores in shale.

3.2.3. FE-SEM. The samples were made into blocks of 6 mm × 6 mm × 6 mm and cut by an argon-ion profiler to obtain a flatter polished section as an observation surface under an electron microscope to improve the observation efficiency of nanopores. The FEI Quanta 650 FEG scanning electron microscope was used to observe and collect microscopic images of shale with a resolution of up to 1.0 nm. At the same time, energy-dispersive X-ray spectroscopy was also used to identify minerals and organic matter and obtain information on shale pore types and organic petrography.

3.2.4. Shale Gas Content Test. The shale gas content test was conducted using FCG006 and FCG009 according to the Chinese industry standard (SY/T6940-2013). The experiment was conducted at a formation temperature of 60°. The total gas content of shale was obtained by adding the contents of analytical gas, lost gas, and residual gas.

4. RESULTS

4.1. Division Scheme of Lithofacies. As the key parameters to control the pore structure, gas content, and mechanical properties of shale,[27−29] mineral components and
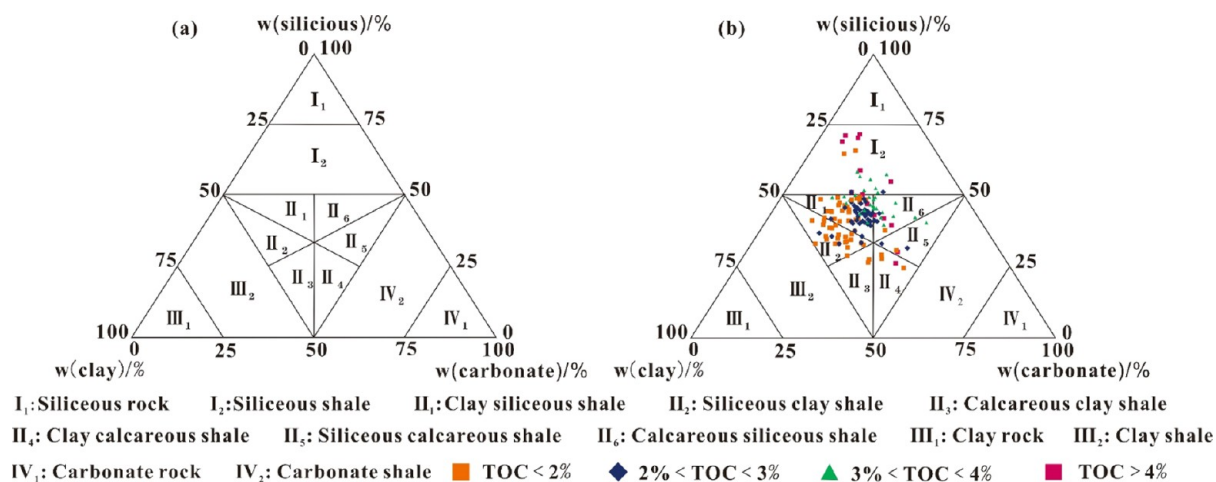
Figure 2. Types of shale lithofacies in Wufeng Formation-Member 1 of Longmaxi Formation in the study area. (a) Division scheme of lithofacies (reprinted with permission from Wang et al.[30]). (b) Triangular diagram of shale mineral composition.
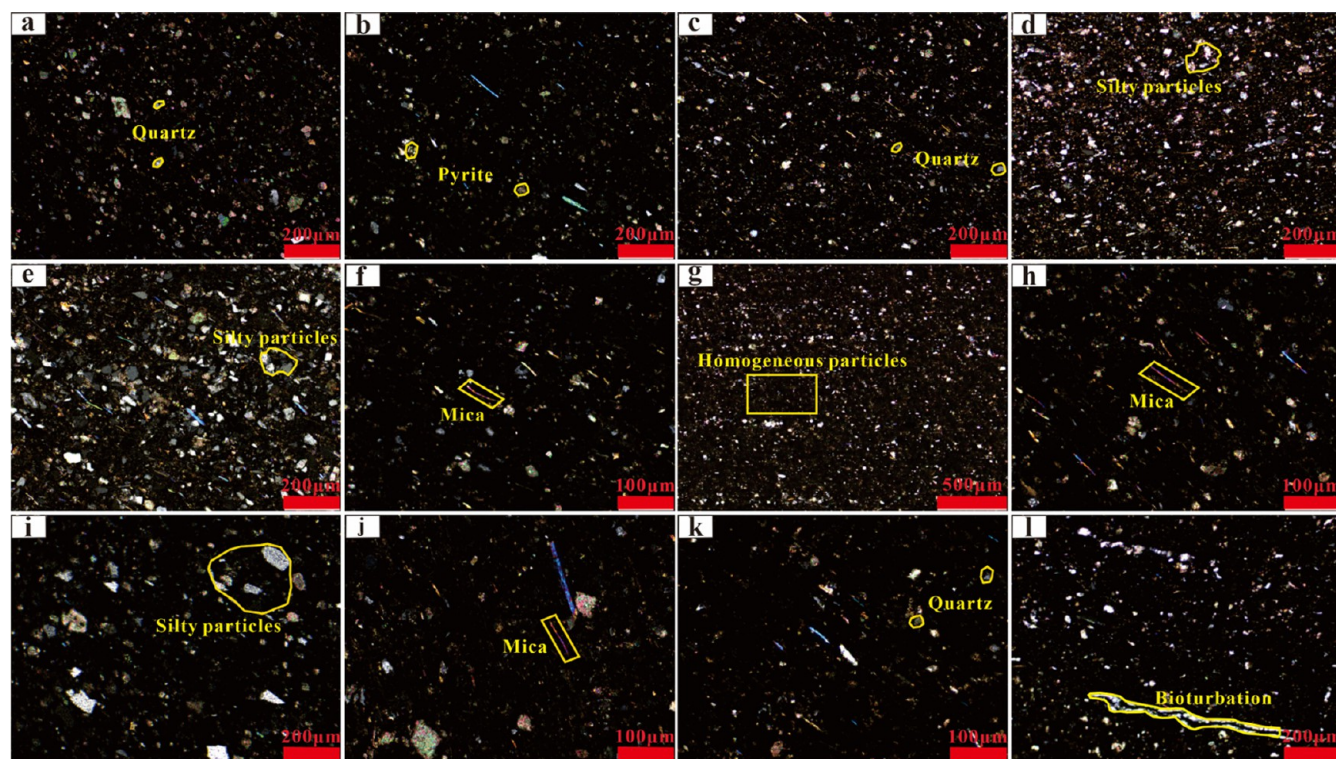

Figure 3. Thin section photographs of different shale lithofacies. (a) High-carbon siliceous shale, 1084.75 m, well Y103; (b) medium-carbon siliceous shale, 1243.05 m, well Y107; (c) medium-carbon clay siliceous shale, 1071.50 m, well Y103; (d) low-carbon clay siliceous shale, 1061.70 m, well Y103; (e) ultra-low-carbon clay siliceous shale, 1032.80 m, well Y103; (f) low-carbon siliceous clay shale, 1218.69 m, well Y107; (g) ultra-low-carbon siliceous clay shale, 1043.57 m, well Y103; (h) ultra-low-carbon calcareous clay shale, 1107.61 m, well Y104; (i) high-carbon clay calcareous shale, 1086.70 m, well Y103; (j) low-carbon siliceous calcareous shale, 1041.72 m, well Y103; (k) medium-carbon calcareous siliceous shale, 1083.30 m, well Y103; and (l) low-carbon calcareous siliceous shale, 1028.50 m, well Y103.

TOC can be obtained accurately by experiments. The lithofacies division scheme is as follows.

4.1.1. Divide the Lithofacies Types Based on the Mineral Components. Based on the difference of mineral components, the three-end-member method (siliceous minerals, carbonate minerals, and clay minerals) is used to divide the lithofacies types. The lithofacies of mountain shale in the complex structural area of northern Yunnan−Guizhou are dominated by mixed shale lithofacies (the contents of siliceous minerals, clay minerals, and carbonate minerals are all ranged from 25 to

50%).[16,17] In this paper, the division scheme of shale lithofacies is appropriately modified (Figure 2a).[30] The division scheme of mixed lithofacies is refined in combination with the mineral components of mountain shale in the study area. In this scheme, the mixed lithofacies are divided into siliceous clay shale (25% < carbonate minerals < siliceous minerals < clay minerals < 50%), clay siliceous shale (25% < carbonate minerals < clay minerals < siliceous minerals < 50%), calcareous siliceous shale (25% < clay minerals < carbonate minerals < siliceous minerals < 50%), siliceous calcareous shale (25% < clay minerals < siliceous

Table 1. Mineral Components of Shale Lithofacies in the Study Area[a]

lithofacies		samples numbers and proportion/%			siliceous minerals/%			carbonate minerals/%			clay minerals/%	TOC/%
type	TOC rank				quartz	feldspar	total	calcite	dolomite	total		
I₂	ultra-low	3	1.9	13.6	36.4−45.3/42.1	13.6−17.5/16.0	50.0−62.1/58.0	6.2−11.1/8.3	3.4−7.2/4.9	9.6−18.3/13.2	20.2−29.5/24.6	0.40−0.68/0.50
	low	3	1.9		40.6−43.1/41.2	4.7−5.5/5.1	45.8−47.8/50.1	11.9−13.6/13.0	18.9−28.6/25.0	17.2−24.4/20.2	18.9−27.4/25.0	2.73−2.96/2.85
	medium	8	5.2		44.2−52.3/47.9	2.5−5.2/4.0	48.1−55.7/51.9	9.1−15.9/13.5	15.9−28.2/22.7	15.8−24.9/20.8	15.9−28.2/22.7	3.01−3.98/3.37
	high	7	4.5		42.1−68.7/56.5	1.0−7.4/4.7	48.2−69.7/61.3	3.4−16.9/7.9	16.8−25.9/20.4	6.8−26.9/14.1	16.8−25.9/20.4	4.02−5.60/5.08
II₁	ultra-low	25	16.13	49.7	25.3−38.6/32.7	5.9−16.4/11.0	32.4−48.5/43.7	9.1−22.6/13.1	2.1−12.4/6.7	11.2−30.8/19.8	27.0−40.2/34.0	0.55−1.97/0.96
	low	40	25.81		31.1−43.1/37.0	2.3−6.2/3.9	34.8−47.2/40.9	12.3−20.6/17.1	4.2−11.8/7.0	16.9−28.4/24.1	26.4−38.3/30.1	2.00−2.95/2.55
	medium	11	7.1		35.5−44.8/40.7	2.1−5.2/3.8	38.9−48.3/44.5	8.7−17.5/13.8	4.3−10.9/7.7	13.2−27.2/20.8	24.8−33.6/28.8	3.18−3.63/3.35
	high	1	0.7		44.3−44.3/44.3	2.7−2.7/2.7	47.0−47.0/47.0	12.0−12.0/12.0	13.0−13.0/13.0	25.0−25.0/25.0	27.4−27.4/27.4	4.98−4.98/4.98
II₂	ultra-low	22	14.19	17.4	25.9−33.6/29.6	2.2−8.1/4.4	28.1−40.1/34.0	9.4−24.7/17.8	0.8−14.2/4.9	12.3−30.6/21.7	24.8−47.4/39.7	0.34−1.9/1.05
	low	5	3.2		24.8−29.2/27.7	3.9−6.8/5.0	31.6−34.8/32.7	7.8−18.8/13.8	4.2−14.5/9.5	15.2−29.2/23.3	34.3−42.1/38.5	2.02−2.76/2.37
II₃	ultra-low	2	1.3	1.3	20.2−23.9/22.1	3.4−6.2/4.8	26.4−27.3/26.9	23.0−30.8/26.9	4.4−11.8/8.1	34.8−35.2/35.0	36.2−37.1/36.7	0.61−0.64/0.63
II₄	ultra-low	3	1.9	2.6	20.6−24.7/23.3	3.3−3.8/3.0	24.4−27.7/26.6	27.9−41.4/33.6	4.3−10.3/6.4	35.8−45.9/40.0	28.7−32.8/30.7	0.35−0.75/0.57
	high	1	0.7		24.6−24.6/24.6	0.3−0.3/0.3	24.9−24.9/24.9	24.6−24.6/24.6	16.4−16.4/16.4	41.0−41.0/41.0	28.8−28.8/28.8	5.60−5.60/5.60
II₅	ultra-low	1	0.6	2.6	24.7−24.7/24.7	5.3−5.3/5.3	30.0−30.0/30.0	7.7−7.7/7.7	32.2−32.2/32.2	39.9−39.9/39.9	27.0−27.0/27.0	1.70−1.70/1.70
	low	2	1.3		27.1−27.6/27.4	3.1−5.0/4.1	30.7−32.1/31.4	23.2−29.5/26.4	11.4−12.9/12.2	34.6−42.4/38.5	23.7−29.6/26.7	2.75−2.90/2.83
	high	1	0.7		28.3−28.3/28.3	1.1−1.1/1.1	29.4−29.4/29.4	29.7−29.7/29.7	11.0−11.0/11.0	40.7−40.7/40.7	27.2−27.2/27.2	4.30−4.30/4.30
II₆	ultra-low	2	1.3	12.9	26.4−29.8/28.1	11.0−12.6/11.8	37.4−42.4/39.9	11.1−16.1/13.6	17.5−17.9/17.7	28.6−34.0/31.3	27.1−27.3/27.2	0.70−0.81/0.76
	low	4	2.6		34.6−36.6/35.5	4.6−5.7/3.7	39.4−41.1/40.1	17.3−22.9/19.2	4.8−12.3/9.3	27.7−29.6/28.5	24.0−27.4/25.8	2.39−2.80/2.57
	medium	11	7.1		36.0−45.2/39.8	2.3−5.6/3.2	38.4−47.5/43.0	13.4−25.1/16.6	5.9−18.6/12.6	24.6−38.9/29.2	16.0−25.7/22.9	3.09−3.80/3.30
	high	3	2.0		33.1−37.6/35.6	2.6−5.0/4.2	38.1−41.2/39.8	14.4−24.1/17.6	6.6−19.4/13.1	27.6−33.8/30.7	23.6−26.2/24.8	4.20−4.90/4.50

[a]36.4−45.3/42.1 represents min−max/average.

minerals < carbonate minerals < 50%), clay calcareous shale (25% < siliceous minerals < clay minerals < carbonate minerals < 50%), calcareous clay shale (25% < siliceous minerals < clay minerals < carbonate minerals < 50%), and calcareous clay shale (25% < siliceous minerals < carbonate minerals < clay minerals < 50%).

4.1.2. Divide the Lithofacies Sub-types Based on the TOC Content. Further division of lithofacies subtypes on the basis of differences in shale TOC content (Figure 2b). The requirements for shale reservoirs to be the potential industrial exploitation target are TOC ≥ 2.0%; gas content > 2.0 m^3/t.[31] Combining the current situation of mountain shale research in the study area and referring to previous research results,[12] shale lithofacies are subdivided into four types in this paper, using 4.0, 3.0, and 2.0% as TOC division thresholds. These include the high-carbon shale (TOC > 4.0%), medium-carbon shale (TOC between 3.0 and 4.0%), low-carbon shale (TOC between 2.0 and 3.0%), and extra-low-carbon shale (TOC < 2.0%).

4.2. Lithofacies Types and Their Characteristics. *4.2.1. Siliceous Shale (I$_2$).* Under the microscope, the siliceous shale shows an under-uniform distribution of quartz, feldspar, and carbonate fragments, with lamellar aggregates and a small amount of pyrite speckled with a predominantly muddy structure (Figure 3a,b). The TOC content ranges from 0.40 to 5.60%, with the TOC grade being mainly medium-carbon, followed by high-carbon. The lithofacies subtypes mainly consist of (medium-carbon to high-carbon) siliceous shales, which have a high overall hydrocarbon potential. The siliceous mineral mass fraction in the medium-carbon siliceous shale ranges from 48.1 to 55.7%, with an average of 51.9%, and the carbonate mineral mass fraction ranges from 15.8 to 24.9%, with an average of 20.8%. The siliceous mineral mass fraction in the high-carbon siliceous shale ranges from 48.2 to 69.7%, with an average of 61.3%, and the carbonate mineral mass fraction ranges from 6.8 to 26.9%, with an average of 14.1% (Table 1).

4.2.2. Clay Siliceous Shale (II$_1$). Under the microscope, the clay siliceous shale shows fine flaky mica bedding distribution. The feldspar and quartz particles are silt-mud grade, with a particle size of <0.03 mm, and the carbonate particle size is 0.03−0.05 mm (Figure 3c−e). The TOC content is between 0.55 and 4.98%, and the lithofacies subtypes are mainly (ultra-low-carbon to medium-carbon) clay siliceous shales, which have medium hydrocarbon generation potential. The content of siliceous minerals in low-carbon clay siliceous shale is 34.8−47.2%, with an average of 40.9%, and the content of carbonate minerals is 16.9−28.4%, with an average of 24.1%. The content of siliceous minerals in medium-carbon clay siliceous shale is 38.9−48.3%, with an average of 44.5%, and the content of carbonate minerals is 13.2−27.2%, with an average of 20.8% (Table 1).

4.2.3. Siliceous Clay Shale (II$_2$). The feldspar and quartz particles in the siliceous clay shale are sub-angular to round, with a particle size of <0.05 mm, and a small number of particles can reach 0.1−0.18 mm. The organic matter is disseminated in the mud, and the pyrite is granular and has an aggregate distribution (Figure 3f,g). The TOC content is between 0.34 and 2.76%, and the TOC grade is mainly ultra-low carbon, followed by low carbon. The lithofacies subtype is mainly extra-low-carbon siliceous clay shale, and a small amount of low-carbon siliceous clay shale is developed. The hydrocarbon generation potential of lithofacies is generally poor. The siliceous mineral content in the ultra-low carbon siliceous clay shale is 28.1−40.1%, with an average of 34.0%, and the carbonate mineral content is 12.3−

30.6%, with an average of 21.7%. The content of siliceous minerals in low-carbon siliceous clay shale is 31.6−34.8%, with an average of 32.7%, and the content of carbonate minerals is 15.2−29.2%, with an average of 23.3% (Table 1).

4.2.4. Calcareous Clay Shale (II$_3$). The calcareous clay shale shows layered and banded aggregation of quartz, feldspar, and carbonate debris and layered aggregation of pyrite (Figure 3h). The TOC content is between 0.61 and 0.64%, and the lithofacies subtype is ultra-low-carbon calcareous clay shale, which has poor hydrocarbon generation potential. The siliceous mineral content in the ultra-low-carbon calcareous clay shale is 26.4−27.3%, with an average of 26.9%, and the carbonate mineral content is 34.8−35.2%, with an average of 35.0% (Table 1).

4.2.5. Clay Calcareous Shale (II$_4$). Feldspar and quartz particles are locally enriched in the clay calcareous shale under the microscope, which are interbedded with shale. The size of carbonate particles is 0.02−0.07 mm, and the organic matter is distributed in small clumps, with granular and strawberry pyrite (Figure 3i). The TOC content is 0.35−5.60%, and the TOC grade is mainly extra-low-carbon, followed by high-carbon. The lithofacies subtype is mainly ultra-low-carbon clay calcareous shale, which has poor hydrocarbon generation potential. The siliceous mineral content in the ultra-low-carbon clay calcareous shale is 24.4−27.7%, with an average of 26.6%, and the carbonate mineral content is 35.8−45.9%, with an average of 40.0% (Table 1).

4.2.6. Siliceous Calcareous Shale (II$_5$). The siliceous calcareous shale occasionally sees fine flaky mica under the microscope. Silt-grade quartz and feldspar particles are evenly distributed. The particle size is mostly <0.05 mm, and the carbonate particle size is 0.02−0.05 mm (Figure 3j). The TOC content is between 1.70 and 4.30%. The TOC grade is mainly low-carbon, and the lithofacies subtype is mainly low-carbon siliceous calcareous shale, which has low hydrocarbon generation potential. The content of siliceous minerals in low-carbon siliceous calcareous shale is 30.7−32.1%, with an average of 31.4%, and the content of carbonate minerals is 34.6−42.4%, with an average of 38.5% (Table 1).

4.2.7. Calcareous Siliceous Shale (II$_6$). The particle size of feldspar and quartz in calcareous siliceous shale is less than 0.03 mm, and the particle size of carbonate is 0.02−0.06 mm (Figure 3k,l). The TOC content is between 0.70 and 4.90%, and the TOC grade is mainly medium-carbon, followed by low-carbon and high-carbon. The lithofacies subtypes are mainly (low-carbon to high-carbon) calcareous siliceous shale, and a small amount of ultra-low-carbon calcareous siliceous shale is developed. The siliceous mineral content in the medium-carbon calcareous siliceous shale is 38.4−47.5%, with an average of 43.0%, and the carbonate mineral content is 24.6−38.9%, with an average of 29.2%. The content of siliceous minerals in low-carbon calcareous siliceous shale is 39.4−41.1%, with an average of 40.1%, and the content of carbonate minerals is 27.7−29.6%, with an average of 28.5%. The content of siliceous minerals in high-carbon calcareous siliceous shale is 38.1−41.2%, with an average of 39.8%, and the content of carbonate minerals is 27.6−33.8%, with an average of 30.7% (Table 1).

4.3. Reservoir Characteristics. *4.3.1. Characteristics of Laminate Development.* The laminate structure is the smallest sedimentary unit widely developed in shale, with a single layer thickness of less than 10 mm.[32−34] On the basis of thin section and core analysis, the high-carbon siliceous shale has a high degree of development of laminates, mainly the silt laminates, with a density of 6−12 laminates/cm and a thickness of 0.25−
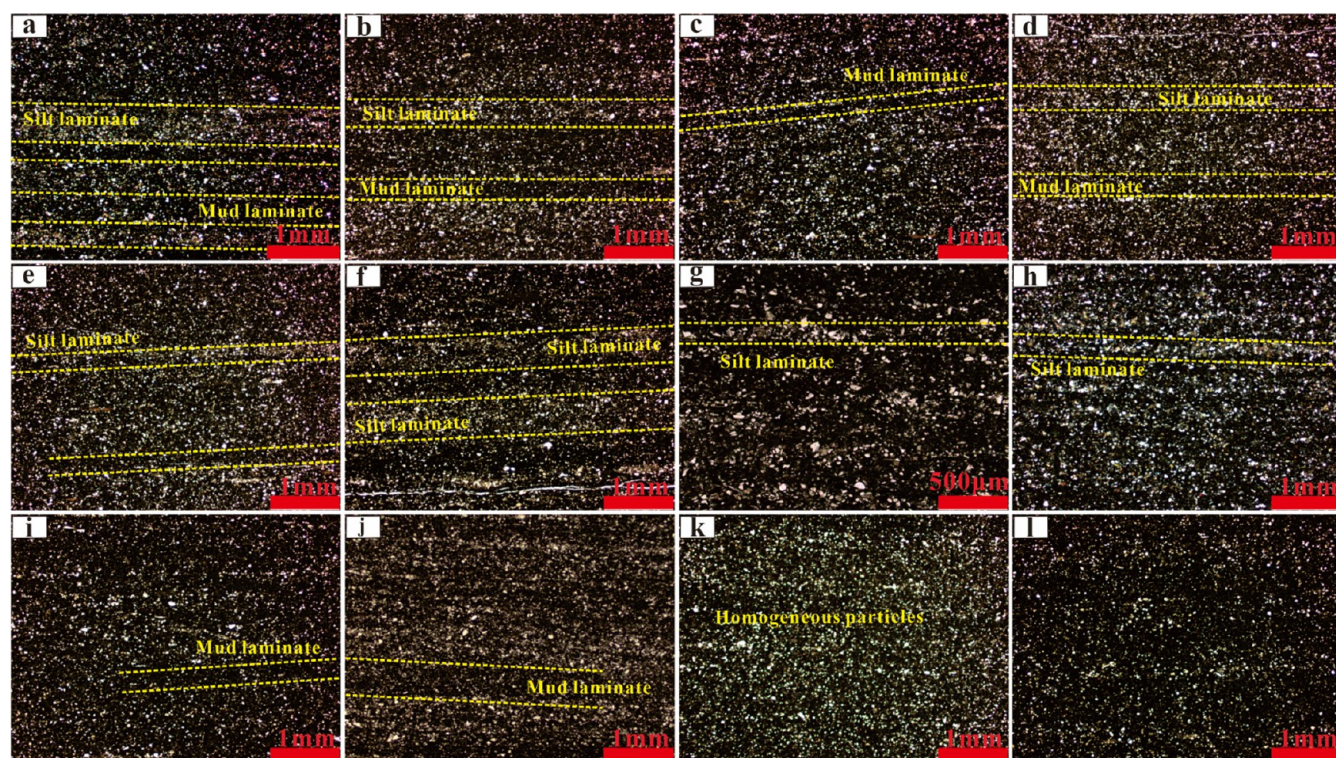
Figure 4. Laminate characteristics of main developed shale lithofacies. (a) High-carbon siliceous shale with developed horizontal laminates, 1642.50 m, well YS203; (b) medium-carbon siliceous shale with horizontal laminates, 1243.05 m, well Y107; (c) medium-carbon clay siliceous shale, 1064.30 m, well Y104; (d) low-carbon clay siliceous shale, 1668.52 m, well Y105; (e) medium-carbon calcareous siliceous shale, 1081.40 m, well Y103; (f) medium-carbon calcareous siliceous shale, 1638.40 m, well YS203; (g) low-carbon siliceous clay shale, 1210.85 m, well Y107; (h) low-carbon calcareous siliceous shale, 1678.20 m, well Y105; (i) ultra-low-carbon clay siliceous shale, 1039.19 m, well Y103; (j) ultra-low-carbon clay siliceous shale, 1030.39 m, well Y103; (k) ultra-low-carbon siliceous clay shale, 1055.90 m, well Y103; and (l) ultra-low-carbon calcareous siliceous shale, 1070.62 m, well Y103.

0.80 mm (Figure 4a). The medium-carbon siliceous shale silt laminates and mud laminates are both developed, with an average density of 6 laminates/cm and a thickness of 0.10−0.60 mm (Figure 4b). The low-carbon to medium-carbon clay siliceous shale has both silt and mud laminates, but with lower laminates density and thickness (Figure 4c,d). The medium-carbon calcareous siliceous shale has silt laminates with occasional discontinuous laminates, with a density of 4−8 laminates/cm and a thickness of 0.20−0.80 mm (Figure 4e,f). The low-carbon siliceous clay shales (Figure 4g) and low-carbon calcareous siliceous shales (Figure 4h) develop silt laminates with a low density. Occasional discontinuities are seen in the extra-low-carbon clay siliceous shales (Figure 4i,j). The extra-low-carbon siliceous clay shale (Figure 4k) and the extra-low-carbon calcareous siliceous shale (Figure 4l) lack the development of laminates.

4.3.2. Pore Types and Physical Properties of Reservoir. The study of shale reservoir pore types is the basis of shale reservoir evaluation.[35,36] The pore size of shale is small, and the pore morphology and genesis are diverse. The micro−nano connected pores and micro-fractures together form a pore network for gas occurrence and seepage.[37−39] The mountain shales in the study area mainly develop intergranular pores and organic pores. The organic pores of the high-carbon siliceous shales are very well developed, with a predominantly rounded and subrounded morphology (Figure 5a,b), pore size usually greater than 100 nm, good connectivity, and an average porosity of 5.0% (Table 2). The medium-carbon siliceous shales show micro fractures at the mineral margins and dissolved pores

within the particles, with small organic pore sizes (Figure 5c,d) and slightly poorer connectivity, with an average porosity of 4.4%. The medium-carbon clay siliceous shale has a strip of organic matter, with organic pores and dissolution pores at the mineral margins (Figure 5e,f), most of which are between 50 and 100 nm in size, with slightly poor connectivity and an average porosity of 4.2%. The low-carbon calcareous siliceous shale is low in organic matter, developing organic pores and micro fractures (Figure 5g,h), with small organic pore sizes and low porosity, with an average porosity of 1.28%. Extra-low-carbon clay siliceous shales and extra-low-carbon siliceous clay shales occasionally show micro fracture development (Figure 5l). Pyrite intergranular pores are found within strawberry pyrite, with irregular polygonal pore morphology and pore sizes ranging from tens to hundreds of nanometers (Figure 5i), organic and inorganic pores are both poorly developed (Figure 5j,k) with porosity averages of 4.5 and 4.0%, respectively.

4.3.3. Pore Volume and Specific Surface Area. N_2 gas adsorption experiments can characterize microscopic pore structure parameters such as specific surface area, pore volume, and mean pore diameter of shale pores.[40,41] The high-carbon siliceous shale in the study area has a large specific surface area and pore volume, while the pore size is small, with an average pore specific surface area of 28.55 cm^2/g, an average pore volume of 0.0397 cm^3/g, and an average pore diameter of 8.90 nm (Table 2). The medium-carbon siliceous shale pores have an average specific surface area of 24.35 cm^2/g, an average pore volume of 0.0363 cm^3/g, and an average pore diameter of 9.73 nm. The medium-carbon clay siliceous shale has a similar
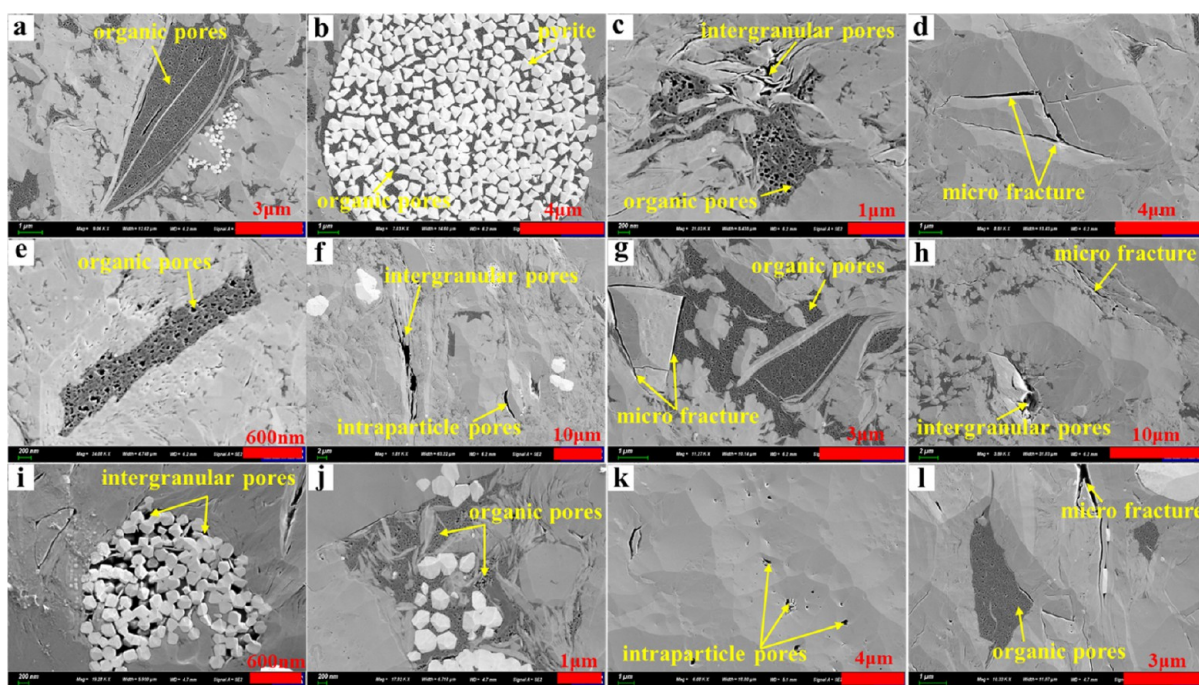
Figure 5. Pore types of main developed shale lithofacies. (a) High-carbon siliceous shale, 1640.75 m, well YS203; (b) high-carbon siliceous shale, 1640.75 m, well YS203; (c) medium-carbon siliceous shale, 1636.15 m, well YS203; (d) medium-carbon siliceous shale, 1636.15 m, well YS203; (e) medium-carbon clay siliceous shale, 1632.80 m, well YS203; (f) medium-carbon clay siliceous shale, 1632.80 m, well YS203; (g) low-carbon calcareous siliceous shale, 1644.10 m, well YS203; (h) low-carbon calcareous siliceous shale, 1644.10 m, well YS203; (i) ultra-low-carbon clay siliceous shale, 1622.65 m, well YS203; (j) ultra-low-carbon clay siliceous shale, 1622.65 m, well YS203; (k) ultra-low-carbon siliceous clay shale, 1612.99 m, well YS203; and (l) ultra-low-carbon siliceous clay shale, 1612.99 m, well YS203.

Table 2. TOC, Total Gas Content, and Pore Structure Parameters of the Main Developed Shale Lithofacies in the Study Area

lithofacies		pore structure parameters					
type	TOC rank	specific surface area/(m^2/g)	pore volume/(mL/g)	pore diameter/nm	porosity/%	total gas content/(m^3/t)	TOC/%
I$_2$	medium	24.35	0.0363	9.73	4.41	2.68	3.37
	high	28.55	0.0397	8.90	5.03	3.17	5.08
II$_1$	ultra-low	20.66	0.0359	9.79	4.52	1.66	0.96
	low	23.52	0.0374	9.55	3.19	2.09	2.55
	medium	25.44	0.0371	9.34	4.23	2.99	3.35
II$_2$	ultra-low	21.11	0.0361	9.84	3.97	1.54	1.05
	low	22.44	0.0283	8.06	4.17	1.56	2.37
II$_6$	low	21.90	0.0340	9.90	1.28	1.67	2.57
	medium	23.40	0.0320	9.00	3.09	3.04	3.3

cumulative average specific surface area and pore volume to the medium-carbon siliceous shale, with an average pore specific surface area of 25.44 cm^2/g, an average pore volume of 0.0371 cm^3/g, and an average pore size of 9.34 nm. The medium-carbon clay siliceous shales and the medium-carbon and high-carbon siliceous shales boast significant specific surface areas and pore volumes, which can provide sufficient sorption sites and storage space for shale gas accumulation. The average pore specific surface area of the low-carbon calcareous siliceous shale, the extra-low-carbon clay siliceous shale, and the extra-low-carbon siliceous clay shale is the smallest, with mean values of 21.90, 20.66, and 21.11 cm^2/g. The cumulative pore volume is quite low, with mean values of 0.0340, 0.0359, and 0.0361 cm^3/g. The average pore sizes are all small, at 9.90, 9.79, and 9.84 nm, respectively, indicating that the microscopic pore structure of this lithological shale reservoir is of poor quality and contributes little to the adsorption and storage of shale gas.

4.3.4. Gas Content. Gas content is an indispensable indicator of shale reservoir capacity and economic recovery value.[42,43] In the study area, the medium-carbon clay siliceous shales and the medium-carbon and high-carbon siliceous shales have higher TOC content, more developed organic pores, and good pore connectivity, resulting in higher gas content, with average values higher than 2.50 m^3/t. The extra-low-carbon clay siliceous shale, low-carbon calcareous siliceous shale and extra-low-carbon and low-carbon siliceous clay shale have lower TOC content, less developed organic pores, and lower gas content. Low-carbon calcareous siliceous shales have poor TOC content, poorly developed organic pores, and low gas content, all below 2.0 m^3/t. High-carbon siliceous shales have the highest gas content at 3.17 m^3/t, followed by medium-carbon calcareous siliceous, medium-carbon clay siliceous, and medium-carbon siliceous shales, with gas contents of 3.04, 2.99, and 2.68 m^3/t (Table 2), respectively. The low-carbon siliceous clay shale and the low-carbon calcareous siliceous shale have comparable TOC
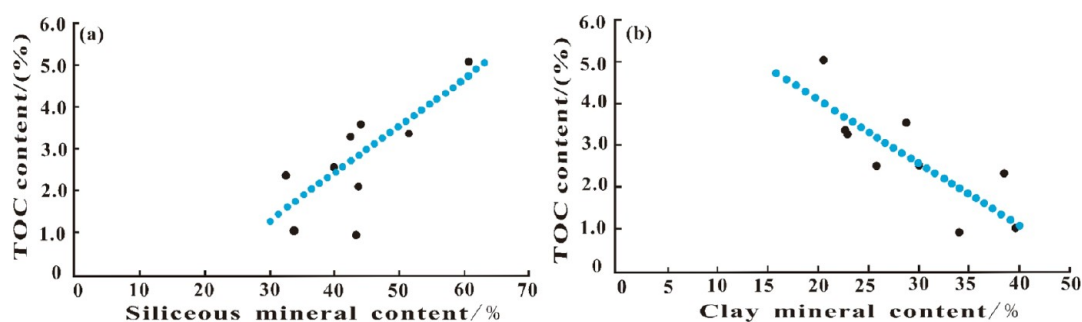
Figure 6. Relationship between TOC content and (a) siliceous mineral content and (b) clay mineral content.
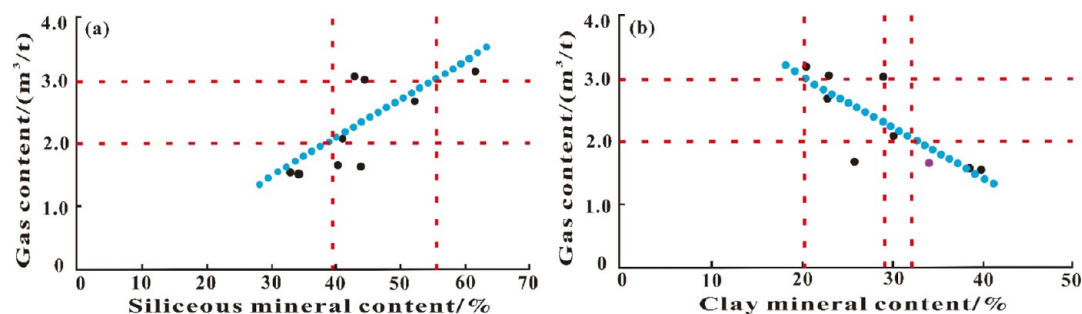

Figure 7. Relationship between total gas content and (a) siliceous mineral and (b) clay mineral content.

Table 3. Classification Standards of Advantageous Lithofacies Shale Reservoir in the Study Area

type	total gas content/(m³/t)	TOC/(%)	siliceous minerals/%	clay minerals/%	lithofacies
I	>3.0	>3.0	>55	<28.0	I_2
II	2.0−3.0	2.0−3.0	40.0−55.0 (or higher than 40)	20.0−32.0 (or lower than 32)	I_2, II_1, II_6

content, but the porosity of the low-carbon siliceous clay shale is much greater than that of the low-carbon calcareous siliceous shale, resulting in a large difference in gas content of 2.09 and 1.67 m³/t.

5. DISCUSSION

5.1. Discrimination Parameters of Advantageous Lithofacies Shale Reservoir. The advantageous lithofacies shale reservoir in the marine phase requires high organic matter content, high brittleness, and low clay mineral content.[44−46] Taking into account the shale geological conditions and engineering development, three key factors, namely, TOC content, siliceous mineral content, and clay mineral content, were preferentially selected in this paper to establish the grading standard for the advantageous lithofacies shale reservoir in the mountain shale of the study area.

5.1.1. TOC Content. TOC has a good positive correlation with siliceous mineral content and a good negative correlation with clay mineral content (Figure 6a,b). The higher the siliceous content and the lower the clay content, the higher the TOC content. At TOC greater than 4.0%, the lithofacies in the study area are mainly siliceous shale; at TOC ranges from 3.0 to 4.0%, the lithofacies are mainly clay siliceous shale, calcareous siliceous shale, and siliceous shale; while at TOC ranges from 2.0 to 3.0%, the shale lithofacies are mainly clay siliceous shale. A condition for a shale reservoir to be a potential target for industrial exploitation is that the TOC is greater than 2.0%,[31] so the lower limit of the TOC content of the advantageous lithofacies shale reservoir in the mountain shale in the study area is 2.0%.

5.1.2. Siliceous Mineral Content. The siliceous content has a good positive correlation with the gas content,[47,48] and the gas content shows an increasing trend as the siliceous content of the shale increases (Figure 7a). As the siliceous content is greater than 40%, the gas content of most shales increases significantly and begins to exceed 2.0 m³/t; when the siliceous content reaches 55%, the gas content of the shale exceeds 3.0 m³/t. The lower limit of siliceous content for the advantageous lithofacies shale reservoir of the mountain shales in the study area is consequently 40%.

5.1.3. Clay Mineral Content. The clay mineral content has a good negative correlation with the gas content (Figure 7b).[49−51] The higher the clay mineral content in the shale, the less brittleness of the shale is conducive to fracturing, thus affecting the generation and development of fractures. The clay mineral content of the main developmental lithofacies in the study area is less than 33% when the gas content exceeds 2.0 m³/t, and less than 28% when the gas content is greater than 3.0 m³/t. Therefore, the upper limit of clay mineral content for the advantageous lithofacies shale reservoir of the mountain shale in the study area is 33%.

5.2. Classification Standards of Advantageous Lithofacies Shale Reservoir. The four evaluation indexes of shale gas content, TOC content, siliceous mineral content, and clay mineral content were integrated to classify the advantageous lithofacies shale reservoir. High-carbon siliceous shale reservoir is the most favorable reservoir for shale gas exploration and development, with specific indicators of gas content > 3.0 m³/t, TOC content > 3.0%, siliceous mineral content > 55.0%, and clay mineral content < 28.0% (Table 3). It is a well-developed, laminated phase with good organic matter distribution and well-preserved organic pores, high brittle mineral content, and strong physical and fracture ability, which are conducive to shale gas
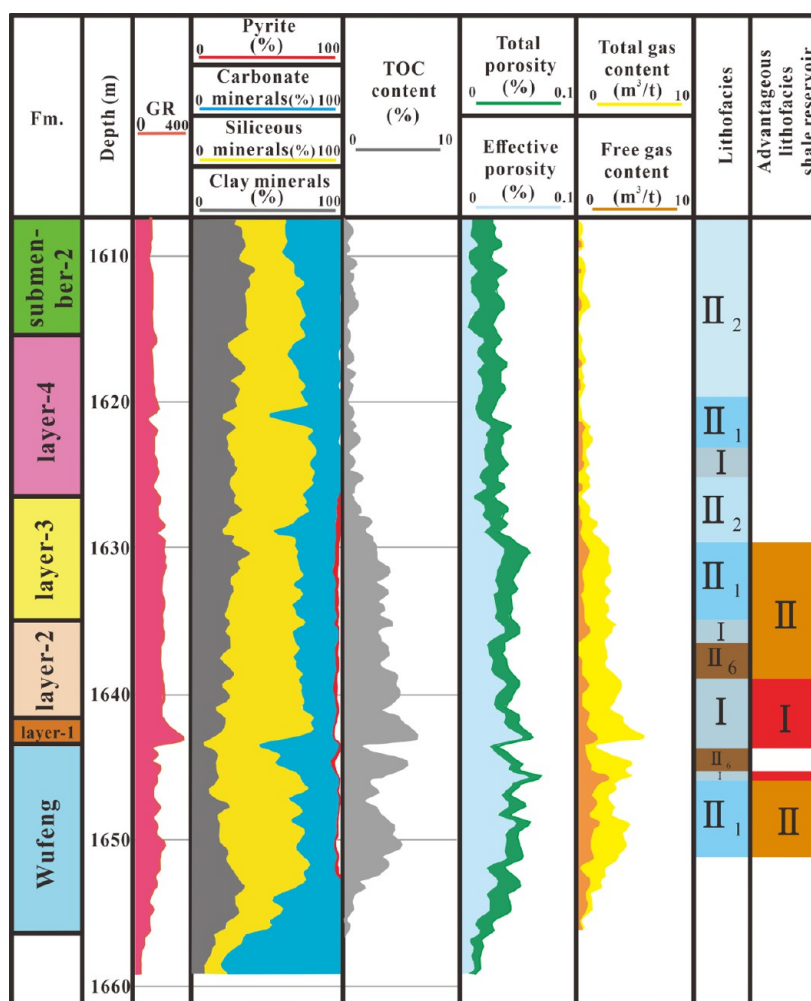
Figure 8. Column showing shale lithofacies characteristics in Wufeng Formation-Member 1 of Longmaxi Formation of well YS203 in the study area.

enrichment and extraction. The medium-carbon siliceous shale, medium-carbon calcareous siliceous shale, and low-carbon and medium-carbon clay siliceous shale reservoir is the second most favorable reservoir for shale gas exploration and development, with specific indicators ranging from 2.0 to 3.0 m³/t gas content, 2.0−3.0% TOC, 40.0−55.0% siliceous minerals (or higher than 40.0%), and 20.0−33.0% clay minerals (or lower than 33.0%). The TOC content of these advantageous lithofacies shale reservoirs is relatively low, the organic matter pore development is slightly poor, and the storage capacity is slightly poor, but they have strong enrichment capacity and fracture ability.

5.3. Advantageous Lithofacies Shale Reservoir Distribution. As an example, well YS203, which has more complete analysis and testing data, has all main lithofacies analyzed in the previous section of the Wufeng Formation−Longmaxi Formation, which is more representative and can reflect the longitudinal development characteristics of the lithofacies. Advantageous lithofacies shale reservoirs are mainly at the bottom of the Wufeng Formation−Longmaxi Formation section. Type I of advantageous lithofacies shale reservoirs is mainly located at layer-1 and the bottom of layer-2 of the Longmaxi Formation, with a thickness of about 4.8 m. Type II of advantageous lithofacies shale reservoirs is located at the top of layer-2 and the bottom of layer-3 of the Longmaxi Formation, with a total thickness of about 14.5 m (Figure 8).

5.4. Influence of the Structure on the Lithofacies Types and Reserve Characteristics. Structural activities play an important role in controlling the accumulation of shale gas, mainly in the control of hydrocarbon generation conditions, reservoir conditions, and preservation conditions.[52] The siliceous shale is mainly formed by biological sedimentation. In the Late Ordovician, volcanic activities provided a large amount of nutrient-rich materials for the outbreak of plankton.[3] At the same time, volcanic eruptions caused the climate environment to change into an anaerobic environment, which was conducive to the preservation of organic matter. Phytoplankton organic debris and clay minerals provide favorable redox conditions for the formation of silicon-rich carbonaceous siliceous shale.[4,53] The shale of Wufeng Formation-Member 1 of Longmaxi Formation in the study area is in deep-water shelf deposition. The maturity of organic matter is between 1.65 and 3.11%, with an average of 2.54%. It is in the over-mature dry gas.[18] A large number of developed organic matter pores can promote the improvement of shale reservoirs. The brittle mineral content in the shale reservoir in the study area is about 30%. When subjected to strong faulting, the brittle minerals in the shale reservoir will deform and dislocate, resulting in the development of large-scale inter-granular pores and micro fractures, which greatly improves the reservoir and permeability of the shale reservoir, and also promotes the conversion of adsorbed gas to free gas. Shale of

submember-2 of Longmaxi Formation in the roof is very dense, with average porosity of 2.8−3.6%, average permeability of 7.7×10^{-8} μm^2, and breakthrough pressure of 17−31 MPa. The nodular limestone of Baota Formation in the floor contacted with the target shale, and the average porosity and permeability were 1.6% and 1.7×10^{-9} μm^2.[2,4] Continuous deposition and large thickness are observed, structural deformation degree is weak, compression-shear fault sealing is good, anticline structure is complete, and shale self-sealing conditions form a complete preservation system which has a positive effect on shale gas storage.

6. CONCLUSIONS

In this paper, the lithofacies of the mountain shale of the Wufeng Formation−Longmaxi Formation in the complex structural area of northern Yunnan−Guizhou are finely divided, the reservoir development characteristics of the main lithofacies are analyzed, and the classification standard of advantageous lithofacies shale reservoir in the study area is established. Advantageous lithofacies shale reservoir that are conducive to exploration and development are clarified and the direction of exploration and development is proposed. Based on the above results, the main conclusions of this study are as follows:

(1) The mountain shale of Wufeng Formation−Longmaxi Formation in the complex tectonic area of northern Yunnan−Guizhou is divided into 7 lithofacies types and 20 lithofacies subtypes, mainly including (ultra-low-carbon to high carbon) siliceous shale, (ultra-low-carbon to high-carbon) clay siliceous shale, (ultra-low-carbon and low-carbon) siliceous clay shale, ultra-low-carbon calcareous argillaceous shale, (ultra-low-carbon and high-carbon) clay calcareous shale, (ultra-low-carbon, low-carbon and high-carbon) siliceous calcareous shale, and (ultra-low-carbon to high-carbon) calcareous siliceous shale.

(2) The organic pores and intergranular pores are mainly developed in the mountain shale in the study area. With the TOC content higher than 2.0%, the development of connected organic pores is higher, the porosity is 3.79% on average, and the physical properties are better. The gas content of the shale is generally higher than 1.0 m³/t, with some higher than 2.0 m³/t, and its distribution characteristics are highly consistent with the TOC content. The main developmental lithofacies such as (medium-carbon and high-carbon) siliceous shale and medium-carbon clay siliceous shale have large specific surface area and pore volume, which can provide sufficient space for shale gas adsorption, storage, and transport.

(3) The high-carbon siliceous shale reservoir of the section of the Wufeng Formation−Longmaxi Formation in the complex structural area of northern Yunnan−Guizhou is mainly located at layer-1 and the bottom of layer-2 of the Longmaxi Formation. The geological and engineering development conditions are the best, and it is the superior shale reservoir for exploration and development in the study area. The medium-carbon siliceous shale and medium-carbon clay siliceous and medium-carbon calcareous siliceous shale reservoir are located at the top of layer-2 and the bottom of layer-3 of the Longmaxi Formation. The TOC content is relatively low, the organic pore development is slightly poor, and the generation and storage capacity are slightly poor, but it

still has a strong shale gas enrichment capacity and fracture ability. These are the second favorable shale reservoirs for shale gas exploration and development in the study area.

(4) During the Late Ordovician-Early Silurian, the strong reduction environment formed by frequent volcanic activities is conducive to the preservation of organic matter, which is the main reason for the development of advantageous lithofacies shale reservoir in the study area. The hydrocarbon generation conditions, reservoir conditions and preservation conditions of shale gas reservoir are excellent due to tectonic action, which leads to good exploration and development potential of shale in the study area.

■ AUTHOR INFORMATION

Corresponding Author
Bingqiang Chai − *School of Geoscience and Technology, Southwest Petroleum University, Chengdu 610500, China;* orcid.org/0000-0001-9255-8308; Email: 1757754665@ qq.com

Authors
Feng Zhao − *School of Geoscience and Technology, Southwest Petroleum University, Chengdu 610500, China*

Yubing Ji − *PetroChina Zhejiang Oilfield Company, Hangzhou 310023, China*

Lei Chen − *School of Geoscience and Technology, Southwest Petroleum University, Chengdu 610500, China;* orcid.org/ 0000-0003-2627-3640

Qingsong Cheng − *PetroChina Zhejiang Oilfield Company, Hangzhou 310023, China*

Complete contact information is available at:
https://pubs.acs.org/10.1021/acsomega.2c05868

Notes
The authors declare no competing financial interest.

■ REFERENCES

(1) Wang, S. Y.; Man, L.; Wang, S. Q.; Wu, L.; Zhu, Y. Q.; Li, Y.; He, Y. F. Lithofacies types, reservoir characteristics and silica origin of marine shales: A case study of the Wufeng formation-Longmaxi Formation in the Luzhou area, southern Sichuan Basin. *Nat. Gas Ind.* **2022**, *9*, 394−410.

(2) Li, L.; Wang, G.; Lian, Z.; Zhang, L.; Mei, J.; He, Y. Deformation mechanism of horizontal shale gas well production casing and its engineering solution: A case study on the Huangjinba Block of the Zhaotong National Shale Gas Demonstration Zone. *Nat. Gas Ind. B* **2018**, *5*, 261−269.

(3) Liang, X.; Xu, Z. Y.; Zhang, Z.; Wang, W.; Zhang, Y.; Lu, H.; Zhang, L.; Zou, C.; Wang, G.; Mei, J.; Rui, Y. Breakthrough of shallow shale gas exploration in Taiyang anticline area and its significance for resource development in Zhaotong, Yunnan Province, China. *Pet. Explor. Dev.* **2020**, *47*, 12−29.

(4) Liang, X.; Zhang, C.; Shan, C. A.; Zhang, J. H.; Wang, W. X.; Xu, Z. X.; Li, Z. F.; Mei, J.; Zhang, L.; Xu, J. B.; Wang, G. C.; Xu, Y. J.; Jiang, L. W. Exploration challenges, countermeasures and prospect of mountain shallow shale gas: A cased study on the Zhaotong National Shale Gas Demonstration Area. *Nat. Gas Ind.* **2021**, *41*, 27−36. (in Chinese)

(5) Chen, W. L.; Zhou, W.; Luo, P.; Deng, H. C.; Qi, M. H. Analysis of the shale gas reservoir in the Lower Silurian Longmaxi Formation, Changxin 1 well, Southeast Sichuan Basin, China. *Acta Pet. Sin.* **2013**, *29*, 1073−1086.

(6) Xu, Z.; Liang, X.; Lu, H.; Zhang, J.; Shu, W. J.; Xu, Y.; Wu, J.; Wang, G.; Lu, W.; Tang, X.; Shi, W. Structural deformation characteristics and shale gas preservation conditions in the Zhaotong National Shale Gas Demonstration Area along the southern margin of the Sichuan Basin. *Nat. Gas Ind.* **2020**, *7*, 224−233.

(7) Zhang, B. M.; Chen, X. H.; Cai, Q. S.; Chen, L.; Zhang, G. T.; Li, P. J. Advantageous gas shale lithofacies of Wufeng Formation-Longmaxi Formation in Yichang slope field of Western Hubei Province, China. *Geol. China* **2022**, *49*, 943−955. (in Chinese)

(8) Wang, C.; Zhang, B.; Lu, Y.; Shu, Z.; Lu, Y.; Bao, H.; Meng, Z.; Chen, L. Lithofacies distribution characteristics and its controlling factors of shale in Wufeng Formation-Member 1 of Longmaxi Formation in the Jiaoshiba area. *Pet. Res.* **2018**, *3*, 306−319.

(9) He, J.; Zhu, S.; Shi, X.; Zhao, S.; Cao, L.; Pan, S.; Wu, F.; Wang, M. Characteristics of Lithofacies in Deep Shale Gas Reservoirs in the Southeast Sichuan Basin and Their Influence on Pore Structure. *Front. Earth Sci.* **2022**, *10*, 857343.

(10) Wang, Z.; Chen, L.; Chen, D.; Lai, J.; Deng, G.; Liu, Z.; Wang, C. Characterization and evaluation of shale lithofacies within the lowermost Longmaxi-Wufeng Formation in the Southeast Sichuan Basin. *J. Pet. Sci. Eng.* **2020**, *193*, 107353.

(11) Chen, S.; Zhang, S.; Wang, Y.; Tan, M. Lithofacies types and reservoirs of Paleogene fine-grained sedimentary rocks Dongying Sag, Bohai Bay Basin, China. *Pet. Explor. Dev.* **2016**, *43*, 218−229.

(12) Yin, X. P.; Jiang, Y. Q.; Fu, Y. H.; Zhang, X. M.; Lei, Z. A.; Chen, C.; Zhang, H. J. Shale lithofacies and reservoir characteristics of Wufeng Formation-lower Long 1 submember of Longmaxi Formation in western Chongqing. *Lithol. Reservoirs* **2021**, *33*, 41−51. (in Chinese)

(13) Kang, J. H.; Wang, X. Z.; Xie, S. Y.; Zeng, D. M.; Du, Y.; Zhang, R.; Zhang, S. M.; Li, Y. Lithofacies types and reservoir characteristics of shales of Jurassic Da'anzhai member in central Sichuan Basin. *Lithol. Reservoirs* **2022**, *34*, 53−65. (in Chinese)

(14) Allix, P.; Bumham, A.; Fowler, T.; Herron, M.; Symington, B. Coaxing oil from shale. *Oilfield Rev.* **2010**, *22*, 4−15.

(15) Wang, G.; Carr, T. R. Marcellus Shale Lithofacies Prediction by Multiclass Neural Network Classification in the Appalachian Basin. *Math. Geosci.* **2012**, *44*, 975−1004.

(16) Chen, K.; Zhang, T.; Liang, X.; Zhang, C.; Wang, G. Analysis of Shale Lithofacies and Sedimentary Environment on Wufeng Formation-Lower Longmaxi Formation in Dianqianbei Depression. *Acta Sedimentol. Sin.* **2018**, *36*, 743−755 (in Chinese).

(17) Li, M. L.; Tan, X. C.; Li, Y. J.; Zou, C.; Zhang, C.; Wang, G. X. Shale lithofacies classification and evaluation of gas-bearing property: a case study of the Wufeng-Longmaxi Formation in northern Yunnan and Guizhou. *Fault-Block Oil Gas Field* **2021**, *28*, 727−732. (in Chinese)

(18) Liang, X.; Zhang, J. H.; Zhang, H. B.; Xu, Z. Y.; Zhang, D. T.; Zhu, D. X. Major discovery and high-efficiency development strategy of shallow shale gas: a case study of Taiyang shale gas field. *China Pet. Explor.* **2021**, *26*, 21−37 (in Chinese).

(19) Liang, X.; Xu, Z.; Zhang, Z.; Wang, W.; Zhang, J.; Lu, H.; Zhang, L.; Zou, C.; Wang, G.; Mei, J.; Rui, Y. Breakthrough of shallow shale gas exploration in Taiyang anticline area and its significance for resource development in Zhaotong, Yunnan Province, China. *Pet. Explor. Dev.* **2020**, *47*, 12−29.

(20) Wang, P.; Zou, C.; Li, X.; Jiang, L.; Li, Q. Main geological controlling factors of shale gas enrichment and high yield in Zhaotong demonstration area. *Acta Petrol. Sin.* **2018**, *39*, 744−753.

(21) Wu, L.; Hu, D.; Lu, Y.; Liu, R.; Liu, X. Advantageous shale lithofacies of Wufeng Formation-Longmaxi Formation in Fuling gas field of Sichuan Basin, SW China. *Pet. Explor. Dev.* **2016**, *43*, 208−217.

(22) Huang, C.; Xu, T.; Ju, Y.; Zhu, H.; Ju, L.; Li, W. Fracability Evaluation of Shale of the Wufeng-Longmaxi Formation in the Changning Area, Sichuan Basin. *Acta Geol. Sin.* **2019**, *93*, 996.

(23) Wang, C.; Zhang, B.; Shu, Z.; Lu, Y.; Liu, C. Lithofacies types and reservoir characteristics of marine shales of the Wufeng Formation-Longmaxi Formation in Fuling area,the Sichuan Basin. *Oil Gas Geol.* **2018**, *39*, 485−497.

(24) Zhang, Z.; Huang, Y.; Ran, B.; Liu, W.; Li, X.; Wang, C. Chemostratigraphic Analysis of Wufeng and Longmaxi Formation in Changning, Sichuan, China: Achieved by Principal Component and Constrained Clustering Analysis. *Energies* **2021**, *14*, 7048.

(25) Zhao, F.; Dong, Z.; Wang, C.; Zhang, W.; Yu, R. Pore Connectivity Characteristics and Controlling Factors for Black Shales in the Wufeng-Longmaxi Formation, Southeastern Sichuan Basin, China. *Energies* **2022**, *15*, 2909.

(26) Chen, Y.; Tang, H.; Zheng, M.; Li, C.; Zhao, S.; Zhao, N.; Leng, Y. Fractal Characteristics and Significance of Different Pore Types of the Wufeng-Longmaxi Formation, Southern Sichuan Basin, China, Based on N2 Adsorption and Image Analysis. *ACS Omega* **2021**, *6*, 30889−30900.

(27) Li, X.; Cai, J.; Liu, H.; Zhu, X.; Li, J.; Liu, J. Characterization of shale pore structure by successive pretreatments and its significance. *Fuel* **2020**, *269*, 117412.

(28) Liu, B.; Teng, J.; Mastalerz, M.; Schieber, J.; Schimmelmann, A.; Bish, D. Compositional Control on Shale Pore Structure Characteristics across a Maturation Gradient: Insights from the Devonian New Albany Shale and Marcellus Shale in the Eastern United States. *Energy Fuels* **2021**, *35*, 7913−7929.

(29) Liu, D.; Tian, T.; Liang, R.; Yang, F.; Ye, F. Characterization of Shale Pore Structure by Multitechnique Combination and Multifractal Analysis and Its Significance. *Geofluids* **2020**, *2020*, 8896940.

(30) Wang, Y. M.; Wang, S. F.; Dong, D. Z.; Li, X. J.; Huang, J. L.; Zhang, C. C.; Guan, Q. Z. Lithofacies characterization of Longmaxi Formation of the Lower Silurian,southern Sichuan. *Earth Sci. Front.* **2016**, *23*, 119−133 (in Chinese).

(31) Wu, J.; Wang, H. Y.; Shi, Z. S.; Wang, Q.; Zhao, K.; Dong, D. Z.; Li, S. X.; Liu, D. X.; Sun, S. S.; Qiu, Z. Favorable lithofacies types and genesis of marine-continental transitional black shale: A case study of Permian Shanxi Formation in the eastern margin of Ordos Basin, NW China. *Pet. Explor. Dev.* **2021**, *48*, 1315−1328.

(32) Shi, Z.; Qiu, Z.; Dong, D.; Lu, L. U.; Liang, P.; Zhang, M. Lamina characteristics of gas-bearing shale fine-grained sediment of the Silurian Longmaxi Formation of Well Wuxi 2 in Sichuan Basin, SW China. *Pet. Explor. Dev.* **2018**, *45*, 358−368.

(33) Wang, C.; Zhang, B.; Hu, Q.; Shu, Z.; Sun, H.; Bao, H. Laminae characteristics and influence on shale gas reservoir quality of lower Silurian Longmaxi Formation in the Jiaoshiba area of the Sichuan Basin, China. *Mar. Pet. Geol.* **2019**, *109*, 839−851.

(34) Wang, S.; Wang, G.; Huang, L.; Song, L.; Zhang, Y.; Li, D.; Huang, Y. Logging evaluation of lamina structure and reservoir quality in shale oil reservoir of Fengcheng Formation in Mahu Sag, China. *Mar. Pet. Geol.* **2021**, *133*, 105299.

(35) Fu, C. Q.; Zhu, Y. M.; Chen, S. B.; Xue, X. H. Structure and Fractal Characteristics of Nano-Micro Pores in Organic-Rich Qiongzhusi Formation Shales in Eastern Yunnan Province. *J. Nanosci. Nanotechnol.* **2017**, *17*, 5996−6013.

(36) Xie, W. D.; Wang, M.; Wang, X. Q.; Wang, Y. D.; Hu, C. Q. Nano-Pore Structure and Fractal Characteristics of Shale Gas Reservoirs: A Case Study of Longmaxi Formation in Southeastern Chongqing, China. *J. Nanosci. Nanotechnol.* **2021**, *21*, 343−353.

(37) Liu, B.; Sun, J.; Zhang, Y.; He, H. E.; Fu, X.; Yang, L.; Xing, J.; Zhao, X. Reservoir space and enrichment model of shale oil in the first member of Cretaceous Qingshankou Formation in the Changling Sag, southern Songliao Basin, NE China. *Pet. Explor. Dev.* **2021**, *48*, 608−624.

(38) Lu, H.; Tang, H.; Wang, M.; Li, X.; Zhang, L.; Wang, Q.; Zhao, Y.; Zhao, F.; Liao, J. Pore Structure Characteristics and Permeability Prediction Model in a Cretaceous Carbonate Reservoir, North Persian Gulf Basin. *Geofluids* **2021**, *2021*, 8876679.

(39) Wang, M.; Tang, H.; Tang, H.; Liu, S.; Zhang, L.; Zeng, M.; Cheng, Y. Impact of Differential Densification on the Pore Structure of Tight Gas Sandstone: Evidence from the Permian Shihezi and Shanxi Formations, Eastern Sulige Gas Field, Ordos Basin, China. *Geofluids* **2019**, *2019*, 4754601.

(40) Bakshi, T.; Vishal, V. A Review on the Role of Organic Matter in Gas Adsorption in Shale. *Energy Fuels* **2021**, *35*, 15249−15264.

(41) Lu, H.; Zhao, A. K.; Tang, H. M.; Lu, L. Z.; Jiang, L. P. Pore Characterization and Its Controlling Factors in the Wufeng-Longmaxi Shale of North Guizhou, Southwest China. *Energy Fuels* **2020**, *34*, 15763−15772.

(42) He, B.; Jiang, Z.; Peng, L.; Zhuo, L.; Tang, X.; Zhang, D.; Ye, X. Shale reservoir characteristics and its influence on gas content of Wufeng-Longmaxi Formation in the southeastern Chongqing. *Nat. Gas Geosci.* **2014**, *25*, 1275−1283.

(43) Nie, H.; Zhang, J. Shale gas accumulation conditions and gas content calculation: A case study of Sichuan Basin and its periphery in the Lower Paleozoic. *Acta Geol. Sin.* **2012**, *86*, 349−361.

(44) Guo, S.; Zhu, Y. M.; Liu, Y.; Tang, X. Characteristics and Controlling Factors of Nanopores of the Niutitang Formation Shale from Jiumen Outcrop, Guizhou Province. *J. Nanosci. Nanotechnol.* **2021**, *21*, 284−295.

(45) Hou, L.; Luo, X.; Yu, Z.; Wu, S.; Zhao, Z.; Lin, S. Key factors controlling the occurrence of shale oil and gas in the Eagle Ford Shale, the Gulf Coast Basin: Models for sweet spot identification. *J. Nat. Gas Sci. Eng.* **2021**, *94*, 104063.

(46) Qiu, Z.; Zou, C.; Wang, H.; Dong, D.; Lu, L.; Chen, Z.; Liu, D.; Li, G.; Liu, H.; He, J.; Wei, L. Discussion on the characteristics and controlling factors of differential enrichment of shale gas in the Wufeng-Longmaxi formations in south China. *Nat. Gas Geosci.* **2020**, *5*, 117−128.

(47) Fan, C. H.; Zhong, C.; Zhang, Y.; Qin, Q. R.; He, S. Geological Factors Controlling the Accumulation and High Yield of Marine-Facies Shale Gas: Case Study of the Wufeng-Longmaxi Formation in the Dingshan Area of Southeast Sichuan, China. *Acta Geol. Sin.* **2019**, *93*, 536−560.

(48) Xu, Z.; Shi, W.; Zhai, G.; Peng, N.; Zhang, C. Study on the characterization of pore structure and main controlling factors of pore development in gas shale. *Nat. Gas Geosci.* **2020**, *5*, 255−271.

(49) Liang, C.; Jiang, Z.; Cao, Y.; Zhang, J.; Guo, L. Sedimentary characteristics and paleoenvironment of shale in the Wufeng-Longmaxi Formation, North Guizhou Province, and its shale gas potential. *J. Earth Sci.* **2017**, *28*, 1020−1031.

(50) Shi, X.; Luo, C.; Cao, G.; He, Y.; Li, Y.; Zhong, K.; Jiang, W.; Lin, M. Differences of Main Enrichment Factors of S_1l 1 1-1 Sublayer Shale Gas in Southern Sichuan Basin. *Energies* **2021**, *14*, 5472.

(51) Yi, J.; Bao, H.; Zheng, A.; Zhang, B.; Shu, W.; Li, J.; Wang, C. Main factors controlling marine shale gas enrichment and high-yield wells in South China: A case study of the Fuling shale gas field. *Mar. Pet. Geol.* **2019**, *103*, 114−125.

(52) He, S.; Li, H.; Qin, Q.; Long, S. Influence of Mineral Compositions on Shale Pore Development of Longmaxi Formation in the Dingshan Area, Southeastern Sichuan Basin, China. *Energy Fuels* **2021**, *35*, 10551−10561.

(53) Liang, X.; Xu, Z. Y.; Zhang, J. H.; Zhang, Z.; Li, Z. F.; Jiang, P.; Jiang, L. W.; Zhu, D. X.; Liu, C. Key efficient exporation and development technoloiges of shallow shale gas: a case study of Taiyang anticline area of Zhaotong National Shale Demonstration Zone. *Acta Petrol. Sin.* **2020**, *41*, 1033−1048. (in Chinese)